

Article

Effect of Existing Façade's Construction and Orientation on the Performance of Low-E-Based Retrofit Double Glazing in Tropical Climate

Sivanand Somasundaram *, Sundar Raj Thangavelu  and Alex Chong

Experimental Power Grid Centre, Energy Research Institute, Nanyang Technological University, Singapore 627590, Singapore; sundar.rt@ntu.edu.sg (S.R.T.); alex.chong@ntu.edu.sg (A.C.)

* Correspondence: sivanand.s@ntu.edu.sg or sivanand.sm@gmail.com

Received: 14 March 2020; Accepted: 31 March 2020; Published: 17 April 2020



Abstract: This paper investigates the effect of an existing façade's construction (viz. clear/grey/solar film, with and without external shade) and orientation on the performance of low-e (hard coat)-based retrofit double glazing in a tropical climate. The performance of double-glazed façades is characterized by the ability to reduce solar heat gain and the consequent reduction in power consumption of air-conditioning systems. This study involves a real-life test-bedding of a low-e (hard coat)-based retrofit double-glazing façade for a few specific cases—clear glass southeast façade without shade, clear glass southwest façade with external shade, and northwest façade with solar film and external shade. Subsequently, energy modelling simulations were done to analyze other scenarios involving various combinations of façade orientation (north, south, west, and east) and façade material (clear glass, tinted grey glass, clear glass with solar film) with and without external sunshades. The east/west-facing façades had a higher impact on the retrofit solution, and more so when the existing façade was of tinted glass or with solar film. For the case analyzed, with a window-to-wall ratio of 8% (based on overall building envelope), a grey tinted east-facing façade could benefit from annual average HVAC energy savings of up to 5.9%.

Keywords: retrofit double glazing; energy savings; façade direction; test bedding; energy model

1. Introduction

Global warming and climate change mitigations have pushed the energy sectors of all countries to look toward options like renewable energy generation, optimal use of conventional fuels, and efficient consumption of energy. In a tropical region like Singapore, the commercial and residential buildings consume around 50% of total electricity [1]. The building sector is at high precedence over other sectors to improve energy efficiency and reduce power consumption, which has translated into Singapore's national target to retrofit 80% of the existing building stock to meet the Green Mark standard by 2030 [2]. The established and upcoming green building solutions focus on all possible aspects like building design, construction, and operations to reduce power consumption. HVAC and lighting are the predominant electrical loads in commercial buildings. Other than the technology advancements in the lighting and HVAC system and control systems [3], there is a need to address the root cause of the problem such as eliminating or reducing the unnecessary heat gain and lighting. This paper's focus is to investigate the performance of retrofit low-e (hard coat)-based double glazing, when installed over an existing conventional single-layer glass façade, in reducing the external heat gain and the effect on indoor lux levels. The technical significance of the present work is to understand how the various parameters, viz., orientation/facing the direction of the façade, tint of glass (clear/grey), presence/absence of solar film on glass, presence/absence of external sunshades, affect the overall impact or performance of the retrofit double glazing.

2. Façade Types and Characteristics

Building façades are broadly classified as opaque, transparent, and translucent. Opaque façades absorb and reflect incident solar radiation and cannot transfer solar heat gain into the building [4], whereas transparent and translucent façades allow direct solar heat gain into the building [5]. These façades are categorized as active and passive types depending on whether there is a presence of equipment (electrical/mechanical) for heat transmission/removal and or electricity generation [5]. Examples of active façades are building-integrated photovoltaic modules, solar thermal or photovoltaic module with thermal collector (PV/T) and forced ventilation of a double-glazed façade. Examples of passive façades are normal building walls, glazing layers, naturally ventilated double glazing, etc.

Hien et al. [6] conducted a theoretical investigation to study the effects of double-glazed façades on energy consumption, thermal comfort, and condensation for an office in Singapore. The study compared the effect of having a 6 mm heat absorption glass 1 m away from the main façade. It concluded that when the 1 m void/gap between the two façades was naturally ventilated, the double-glazed façade was successful in considerably reducing the cooling loads of the building by up to 9%. Perez-Grande et al. [7] studied the effect of glass properties on the performance of a double skin façade, using ten different glass material combinations for the inner and outer façade, which were 0.9 m apart. It was concluded that by choosing optimal material combinations of glass material, the cooling load can be reduced by one order of magnitude, when accompanied with the external forced ventilation of air into the air gap of the double skin façade. A similar analysis was done to arrive at the right combination of the inner skin and outer skin glass materials, using Thermal Analysis Software (TAS) for the optimal design of a double ventilated façade project at the headquarters of the National Securities Market Commission [8]. The effect of cooling by blowing air through the channel (between the inner and outer glasses) was analyzed by Perez-Grande et al. [7]. Valetin et al. [9] conducted an economic assessment of a fan and nozzle-ventilated system for forced ventilation in the air gap for a double skin façade.

Most of the double-glazing studies discussed above are conventional double-skin façades with a large air gap between the inner and outer layer of typically about 1 m. This type of solution must be designed and planned during the construction of a new building. Moreover, such a solution utilizes a large area and is not practical in cities with high land cost. Thus, alternate retrofit solutions, like installing a secondary layer of glazing over an existing glazing with a small air gap (25–50 mm), which is simple, occupies less space, and is yet effective in reducing cooling loads, are required. Most of the old buildings have normal clear or tinted glass (single glass façade), which (a) increases the heat gain through direct solar transmission and convective/re-radiated thermal heat and (b) increases glare in the building. These factors force occupants to use window curtains and blinds to eliminate glare and subsequently end up using artificial indoor lights. In an economic perspective, integrating an additional layer into the façades for decades-old buildings remains attractive compared to upgrading all façades of existing buildings to a standard double-glazing unit (which comes as one sealed unit, sometimes referred to as insulated glazing unit or IGU). The implementation of a double-glazed façade is straight-forward and takes less time to integrate an additional glass layer with a simple support structure without affecting the building operation. Some of the retrofit studies [10–15] show that glazing plays a critical part in improving the performance of existing buildings toward the net-zero energy building (nZEB) target. Out of the several commonly implemented building retrofit options, upgrading the window type and façade insulation are preferable choices for performance improvement [14]. Some of the options such as replacing single-glazed to double-glazed windows [13] and replacing single clear glass to double grey low-e glazing [16] reduce the cooling load substantially and shows an economic impact with a reasonable payback period. Smith et al. [17] introduced a secondary glazing (or internal storm windows) as an alternative to retrofitted insulated glazing units (IGUs) in existing domestic single-glazed window frames. The lab test results confirm that the secondary glazing increased the resistance values from 0.15 to 0.34–0.57 m² K/W in cold climates.

3. Novelty and Knowledge Gap Addressed

In the current work, we intend to investigate the performance of a novel retrofit solution in which a secondary glazing is added inside the room over the existing glass façade with a non-sealed air gap, as shown in Figure 1. This approach will reduce installation time and costs. However, being a non-sealed air gap, the low-e coating is of hard coat type and is located at position 3 (facing the existing façade). Typically, in a double-glazing unit, which is installed as one sealed unit, the low-e layer is typically at position #2 for tropical climates to reduce heat gain. However, in the proposed solution where a secondary layer is added over an existing glazing, the options available for the low-e layer are positions #3 and #4. To maintain durability of the low-e coating, #3 is preferred for such retrofit installations. It is expected that for tropical climates, #3 may not reduce as much heat gain as in #2. In recent times, such a configuration is in use in winter climates such as Japan, etc., to prevent heat escaping from the room. However, how will this novel retrofit solution perform under tropical climates? Will it reduce the heat gain into the building? The literature on the performance of such a retrofit solution in real buildings in tropical weather is quite limited. The other specific key questions that are currently unanswered in the literature and which need to be addressed are: Which facing or orientation benefits more with installation of the proposed novel retrofit double-glazing façade? What role does the existing façade's glass type play? Does the presence or absence of external sun shades play a significant role in the performance? The answers to these questions are important to analyze the potential retrofit scenarios in an existing building and to make the most appropriate decision (taking into account energy savings, retrofit cost, manpower effort, and installation time).

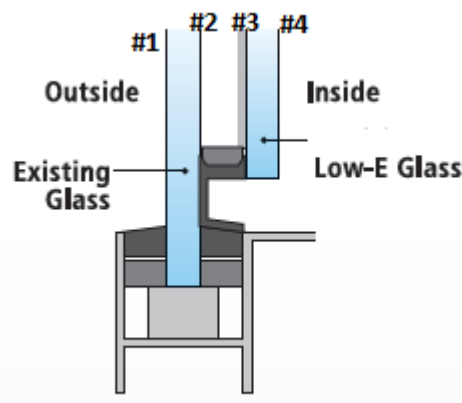


Figure 1. Typical installation of retrofit double glazing.

The current work involved a test-bedding of retrofit low-e (hard coat)-based double-glazing façades for the following configurations: (1) Clear glass in southeast with no sun shade, (2) clear glass in southwest with sunshade, (3) clear glass with solar film and sun shade, where measurements were made before and after the proposed retrofit installation. However, to study the performance under other combinations of orientations and glass types of façade, energy modelling was carried out. The current work is an extension of previous work [18,19]. In the earlier work, a low-e-based retrofit double-glazing test-bedding was conducted for the same room as in this study (which has façades in SE, SW, and NW directions), but the results from the previous work were based on the combined effect of all the three façades. The earlier work [19] highlights the impact of the solar film on the proposed retrofit solution, but the individual effect of façade type and direction needs to be understood and, hence, in the current study, the effect of each façade (material and direction) was studied in isolation.

4. Methodology

The testbed room allowed certain combinations of façade orientations and glass types to be tested; for studying the behavior of other combinations, a simulation model, as described in Section 4.2,

was used. The test bedding experiments served as a real-life demonstration and also helped measure parameters like lux levels, mean radiant temperature, etc., which are difficult to model and measure in simulation models. Moreover, the actual physics of competing effects of increased thermal radiation and lowered direct solar transmission was identified by testbed measurement results, as will be discussed in the Results and Discussion section.

4.1. Description of Test-Bedding

The level 3 room in the office building, which had 3 existing glass façades in the SE, SW, and NW directions, was chosen as the testbed location. The NE direction was covered by an opaque wall. The room orientation is indicated in Figure 2. The length and width of the room were approximately 10.65 and 5.95 m, respectively. The concrete roof was 4.95 m from the floor to ceiling. The height of the plenum space above the false ceiling (drop ceiling formed by gypsum boards) was 1.65 m. The SW and NW façades had fixed metallic aluminum sunshades above the façade, as shown in Figure 2.

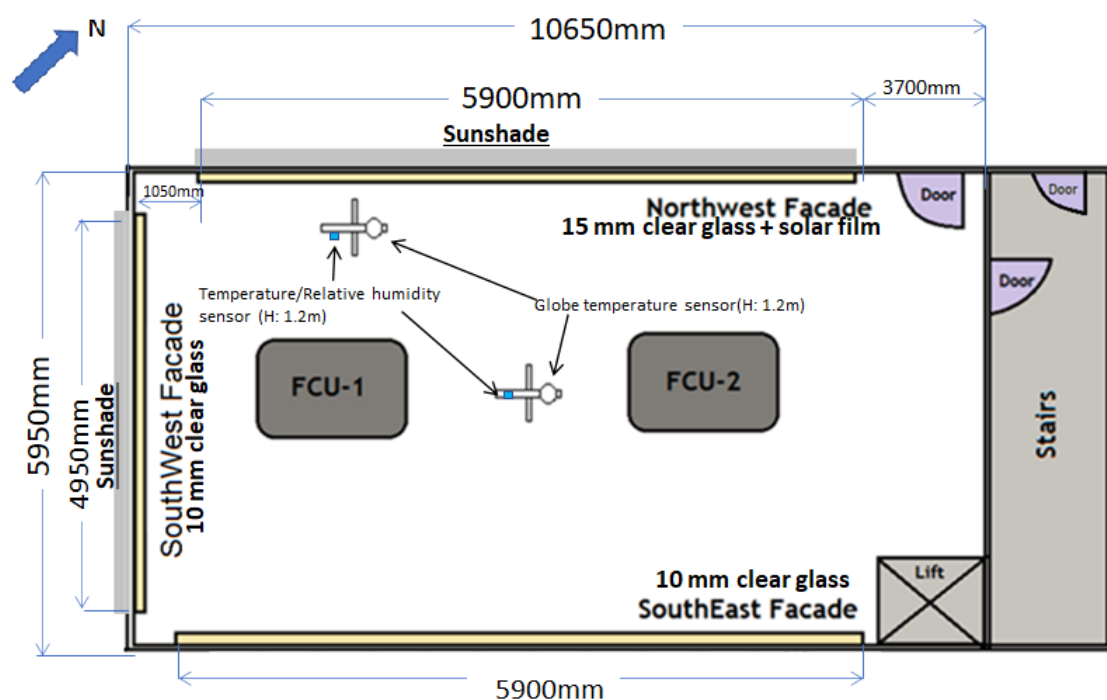


Figure 2. Schematic of room used for test-bedding.

The room was cooled by two individual fan coil units, which had independent compressor/outdoor units. These units were commercial VRF-type HVAC systems. The first unit's fan coil had a cooling capacity of 9.3 kW and the connected compressor had a rated capacity of 11.2 kW for a power consumption of 2.95 kW. The second unit's fan coil had a cooling capacity of 14 kW and the connected compressor had a rated capacity of 14 kW for a power consumption of 3.97 kW. The rated power consumption was for the following scenarios: Indoor room at 27 °C dry bulb temperature and 19.5 °C wet bulb temperature with outside ambient dry bulb temperature at 35 °C. The target setpoint for the room was 25 °C and air-conditioning systems were scheduled to operate from 8 a.m. to 6:30 p.m. The fresh air flow measured at the fresh air duct was 5.7 m/s and it was equivalent to an air change rate of 1 air change per hour (ACH). Singapore Standard 553: 2016 [20] recommends a minimum ACH depending on room size. For the current room being used as the testbed, 0.78 ACH was the required size of this room, and the actual existing fresh air intake was slightly higher at 1 ACH. It is to be noted that the room was in a positive pressurized HVAC system, with the room pressure slightly above the ambient.

The existing three façades differed in a few aspects. The SW and NW had sunshades, but the SE façade did not have any sunshade. In addition, the SE and SW façades were 10 mm thick clear glass, but the NW façade was a 15 mm thick clear glass with a solar film (indicated in Table 1). Table 2 lists the properties of the existing glass façades and the retrofit glass.

Table 1. Properties of existing solar control film in north-west façade.

Properties	Values
Total transmission	9%
Solar energy	
Reflection	20%
Absorption	71%
Visible light	
Transmission	15%
Reflection	11%
Infra-red rejection	75%
Shading coefficient	0.25
Heat transmission (W/m ² K)	5.7

Note: Properties of 0.05 mm IR film over a 6 mm clear glass.

Table 2. Properties of glass façades.

Glass Properties		Clear Glass 10 mm at SE and SW Façade	Clear Glass 15 mm at NW Façade	Sunergy Grey (8 mm with Low-E Hard Coat at Position 2)
Visible light (%)	Transmittance	87	84	26
	Internal Reflection	-	-	4.9
	External Reflection	8	8	8.3
Solar energy (%)	Transmittance	72	58	23.2
	Reflectance	7	7	5.7 (int), 9.4 (ext)
	U value W/m ² K	4.96	4.88	4.1
	Shading coefficient	0.89	0.85	0.41

The retrofit glass (Sunergy grey, AGC) was a hard-coat low-e glass (specifications listed in Table 2). The hard low-e coating on position 3 faced the existing glass façade.

Figure 3 shows the layers in the installed retrofit double-glazing installation for the NW, SW, and SE façades. The low-e coat layer is placed in position 3 facing the existing glass façade. Ideally, the low-e should be in position 2 for the best performance, but in a retrofit solution, position 2 cannot be implemented without complete replacement of the existing glass.

Due to the design of the existing frames in the SE and SW windows, retrofit installation required a new thicker frame and, hence, resulted in an air gap of 30 mm, whereas, in the NW façade, it was maintained at 17 mm. The vertical gaps between the consecutive retrofit glass panels was covered by simple aluminum strips, which were not airtight. The detailed sizes of the glazing and room details like wall thickness, etc., are specified in the earlier work [18].

To test each side of the façade individually, for every test, the other two of the three glass façades remaining were blocked by a temporary wall (built using a partition board with rock wool insulation). The façade that remained uncovered was tested, with measurements of outdoor weather, indoor room conditions, and air-con-related data, as described in Table 3, being recorded before and after the retrofit double-glazing installation. Thus, in summary, there were three pairs of experiments conducted, as listed in Table 4.

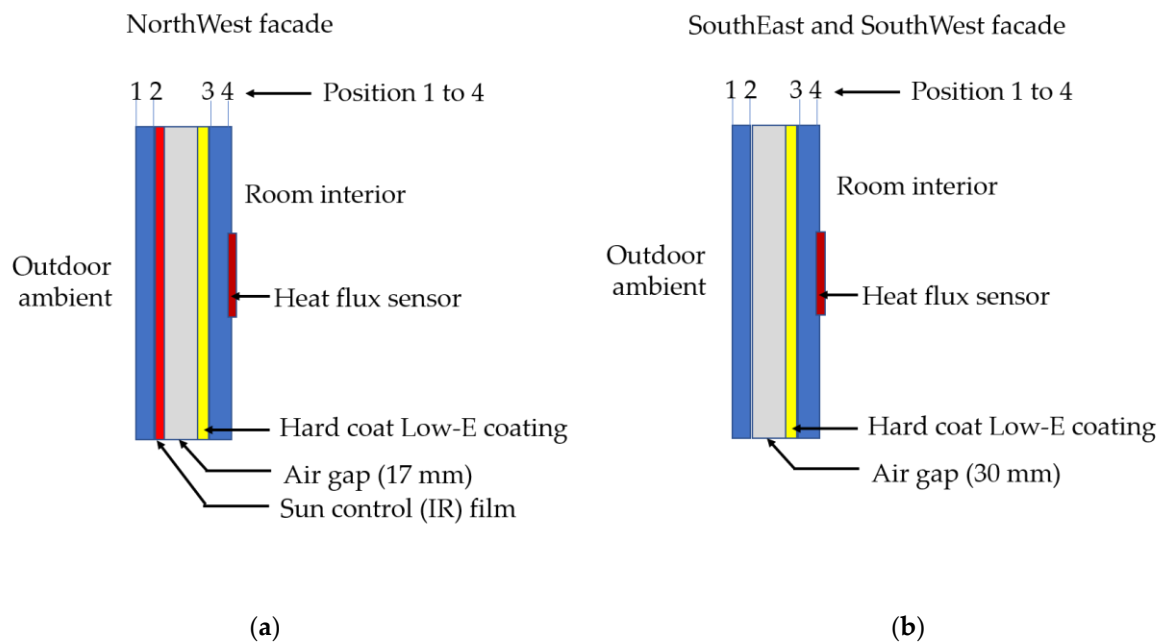


Figure 3. Schematic of installed retrofit glazing system in the NW, SE, and SW façade: (a) NW façade with 17 mm air gap and sun control film; (b) SE and SW façade with air gap of 30 mm.

Table 3. Set of measured parameters with accuracy range.

Sensor Type	Measured Variables	Accuracy
Outdoor Environmental Conditions		
Pyranometer	Global (Total) solar irradiance	$\pm 5\% \pm 10 \text{ W/m}^2$ (hourly)
	Diffuse solar irradiance	$\pm 8\% \pm 10 \text{ W/m}^2$ (individual)
Outdoor Temperature/ Humidity sensor	Dry bulb temperature Relative humidity	$\pm 0.25 \text{ }^\circ\text{C}$ $\pm 1.5\%$
Rain detector	Rain detector (rain=1/no rain=0)	
Outdoor illuminance sensor	Outdoor illuminance	$\pm 3\%$
Room Conditions		
Indoor Temperature/ Humidity sensor	Room temperature Room humidity	$\pm 0.2 \text{ }^\circ\text{C}$ $\pm 1.7\%$
Globe temperature sensor (Pt-100 sensor)	Mean radiant temperature	$\pm 0.1 \text{ }^\circ\text{C}$
lux sensor	Room lux	$1.5\% \pm 2 \text{ lux}$
CO ₂ sensor	Room CO ₂ levels	$\pm 20 \text{ ppm} \pm 1\%$
Pyranometer tilted by 90°	Indoor normal solar irradiance near façade	1.5%
Heat flux sensors	Measure the total heat flux through the façade	$\pm 3\%$
T-type Thermocouple	Façade surface temperatures at existing and new panel	0.75%
Bare junction T type thermocouple	Temperature in the air gap between the panels	0.75%
Air-conditioning operation details		
Digital power meters	Instantaneous and cumulative power consumption of VRF outdoor unit	0.2%
VRF air-conditioning system (In-built sensors)	System status, Air flow speed, direction of return air temperature and temperature setpoint	-

Table 4. Design of experiments.

Aim	Configuration Reference No	Configuration Tested	Testing Date (Start–End)
To study effect of double glazing in SE façade (no solar film no sunshade)	DG	Double glazing in SE + block NW and SW using temporary wall	4-April to 11-April, 2018
	Baseline	Existing glass (single glazing) in SE + block NW and SW using temporary wall	13-April to 26-April, 2018
To study effect of double glazing in SW façade (has sunshade but no solar film)	Baseline	Existing glass (single glazing) in SW + block SE and NW using temporary wall	27-April to 9-May, 2018
	DG	Double glazing in SW + block SE and NW using temporary wall	10-May to 31-May, 2018
To study effect of double glazing in NW direction for a glass with solar film and sunshade	DG	Double glazing in NW (with solar film on base glass) + block SE and SW using temporary wall	2-June to 12-June, 2018
	Baseline	Existing glass (single glazing with solar film) in NW + block SE and SW using temporary wall	13-June to 27-June, 2018

4.2. Description of Simulation Model

Besides the real-life test-bedding, to study other scenarios of different combinations of glass type and orientation with and without shade, an energy simulation model was used. The model was built using Design Builder software. The objective was to calculate the total heat gain into the room from various sources both in the baseline case and in the retrofit double-glazing scenario. The room geometry was the same as the real test-bed room, as shown in Figure 1. However, to make the results more useful, the four sides of the room walls were directly facing north, south, west, and east with zero-degree deviation. For each scenario, all the sides of the rooms were modelled as brick walls, except for the side under investigation, which was modelled to have a glass façade of area 13.8 m² (window-to-wall ratio for this scenario is 8%, calculated based on total window-to-wall area of all four sides). This wall with a glass façade was oriented toward north, south, east, and west to predict the performance in each scenario. Tables 1 and 2 list the glass properties of the baseline glass, solar film, and the retrofit inner window. The fresh air load was taken into consideration by using the measured air change rate in the model. The dehumidification load was modelled by specifying the supply air temperature into the room. The plug loads were also estimated, which arise mainly from instrumentation control panel fans and indoor fan coil units. ASHRAE's (International Weather file for Energy Calculations) IWEC weather file was input for simulation of outdoor weather. More detailed information regarding geometry and material properties can be obtained from our earlier work [18], where the model was validated as well, and the same model has been adapted here to study the effect of façade configuration and direction.

5. Data Collection and Assessment

For the experimental test-bedding, all data were collected at a 1-second sampling frequency. Subsequent data were averaged on an hourly basis. As no two days were exactly identical, they were not directly comparable. However, there were small time periods (of 3 h) that had a higher probability of having similar weather both during the baseline and during the retrofit scenario. It was considered that if any two time periods differ by 0.2 °C or less for the average dry bulb temperature difference between the ambient and room, 0.3 °C or less for the average wet bulb temperature difference between the room and ambient, and also has less than 200 W/m² difference for the average total solar irradiance, they are considered to be comparable to each other. It is noted that to be considered similar, time periods must satisfy all the three parameters stated above (ambient temperature and humidity in

relation to room condition and solar radiation). The detailed discussion of this criterion can be found in our earlier work [18].

6. Results and Discussion

The measurement results of the test-bedding are presented and discussed first. The dominant periods for each façade or tested configuration correspond to the period when the façade directly sees the sun and receives a lot of direct sunshine. This period for different façades is as follows: 9 a.m. to 12 p.m. for SE façade, 12 a.m. to 3 p.m. for SW façade, and 3 p.m. to 6 p.m. for NW façade. The averaged values (during the dominant period) of indoor and outdoor measured values have been tabulated in Table 5, for each configuration both before and after retrofit double glazing.

Table 5. Average (Indoor Environment Quality) IEQ measured during direct sunshine periods for different configurations.

Configuration Time Period (Dominant)	SE Façade 9 a.m.–12 p.m.		SW Façade 12 p.m.–3 p.m.		NW Façade 3 p.m.–6 p.m.	
	Baseline	DG *	Baseline	DG *	Baseline	DG *
Room illuminance (lux)	1454	486	867	112	189	82
Indoor Normal Irradiance (W/m ²)	125	29	40	10	12	8
Façade heat flux into room (W/m ²)	60	130	49	58	120	60
Room panel Temperature (°C)	26.7	37.7	30	32.5	32	35.8
Mean Radiant Temperature (°C)	31.7	30.8	31.5	30.7	31	31.2
Outdoor Illuminance (klux)	53.6	54	66	45	22	39
Ambient Temperature (°C)	30.4	30.4	31.1	29.5	28.8	31.3
Global Solar Irradiance (W/m ²)	517	527	603	428	205	386

DG * refers to double glazing.

For the SE façade, the outdoor ambient conditions, during the baseline tests and after retrofit double-glazing tests, remained almost the same. It is clear that the room panel registered a significant increase in both panel temperature and heat flux entering the room. However, the indoor normal irradiance and mean radiant temperature were lower. The room illuminance levels dropped and reached the recommended range of 320–500 lux levels [21]. There are two competing effects of reduced direct solar transmission and increased re-radiation from the glazing layer. The results observed indicate the mixed effect of these two effects. The SW façade also shows similar trends but the change is moderate and not as drastic as in the SE façade, which can be attributed to the presence of external sun shade over the SW façade, and the angle of the sunrays into this façade is not near-normal (perpendicular) as in the SE façade. The energy stopped by the low-e layer is less and, hence, there is less re-radiation back into the room. For the NW façade, all the parameters—heat flux, indoor irradiance, and lux levels, were significantly reduced after retrofit double-glazing installation, even though the ambient conditions during the retrofit double-glazing installation testing were worse by having higher ambient temperature and higher solar irradiance levels. This positive effect arises from the presence of the solar film in the NW façade in addition to the external sunshade over the NW façade. Though Table 5 gives a quick preview and summary of the different façades tested, the ambient conditions during the baseline and after the double-glazing retrofit were almost same for the SE façade, with a slightly hotter ambient for the SW baseline compared to the SW double-glazed tests, and a slightly cooler ambient for the NW baseline compared to the NW double-glazed tests. Thus, specific one-hour periods with the same/very similar ambient conditions (those which satisfy the tolerance levels as discussed in Section 5) were analyzed and compared in Figures 4–6. Table 6 presents the average energy savings from reduced air-con power consumption after retrofit double glazing. It presents the average values from the comparison of similar time periods, which satisfies the tolerance criterion discussed in Section 5.

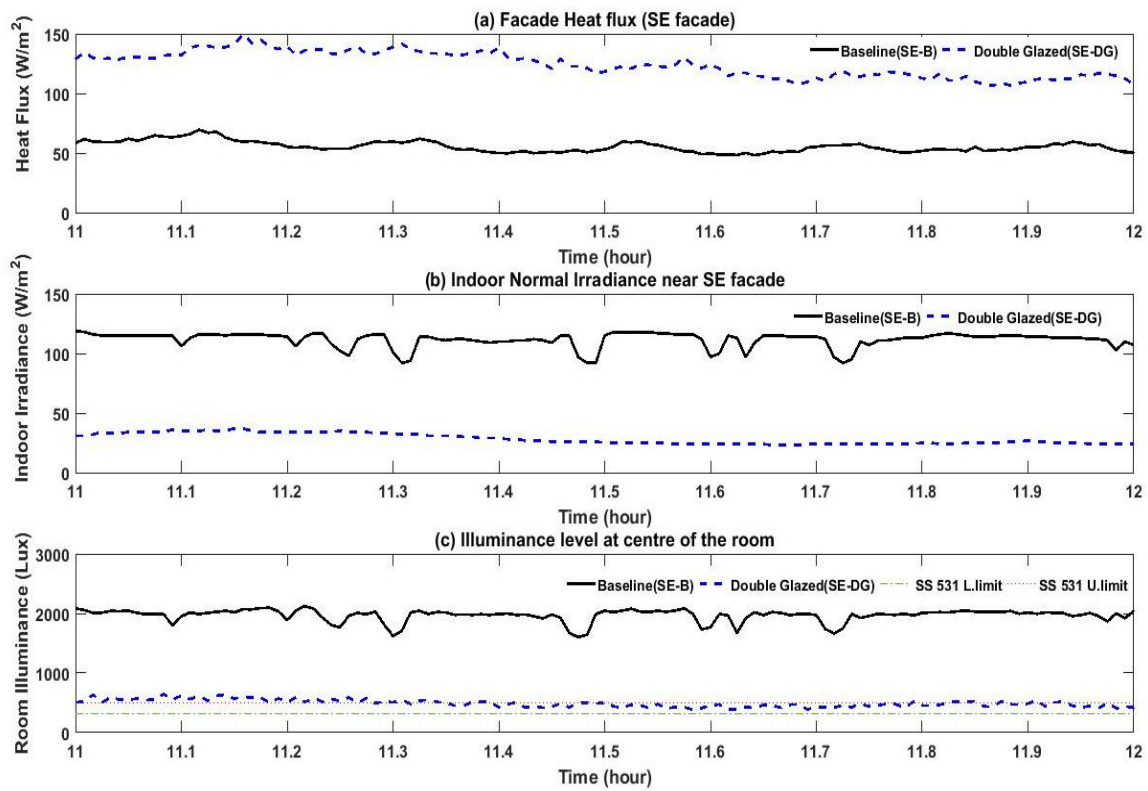


Figure 4. Comparative plots before and after retrofit double glazing of SE façade: (a) Façade heat flux; (b) indoor normal irradiance; (c) illuminance level at room center.

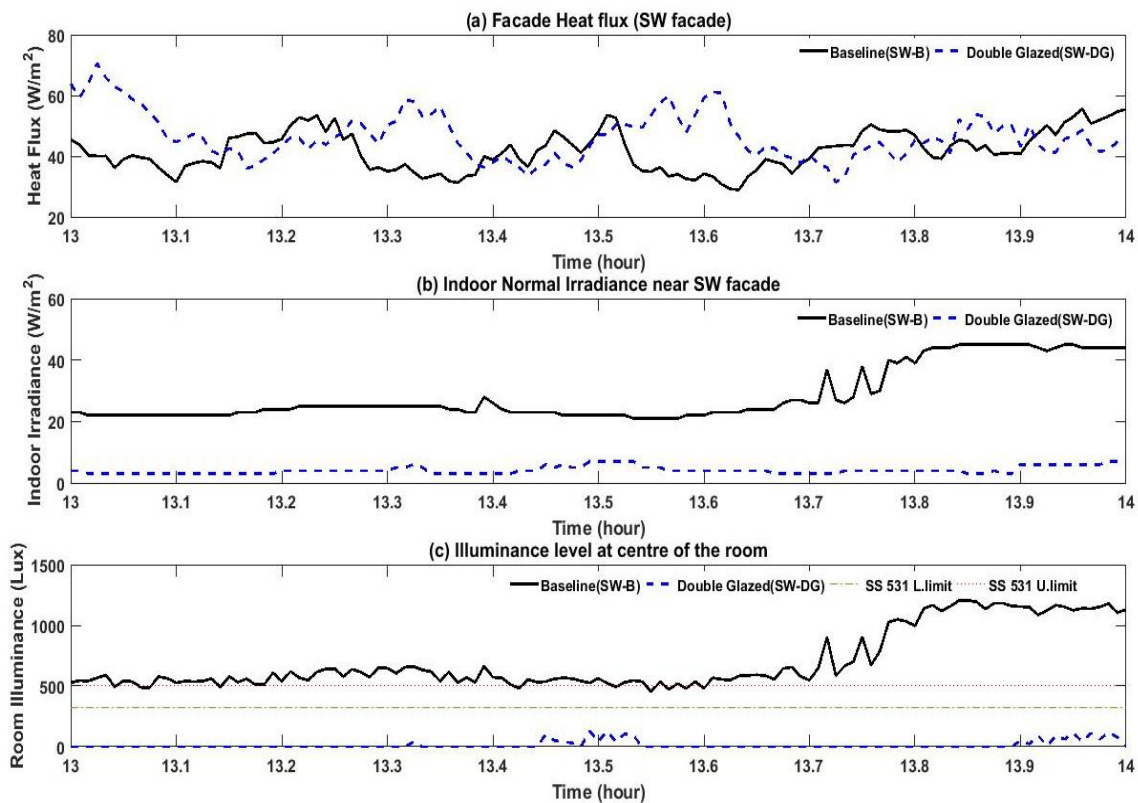


Figure 5. Comparative plots before and after retrofit double glazing of SW façade: (a) Façade heat flux; (b) indoor normal irradiance; (c) illuminance level at room center.

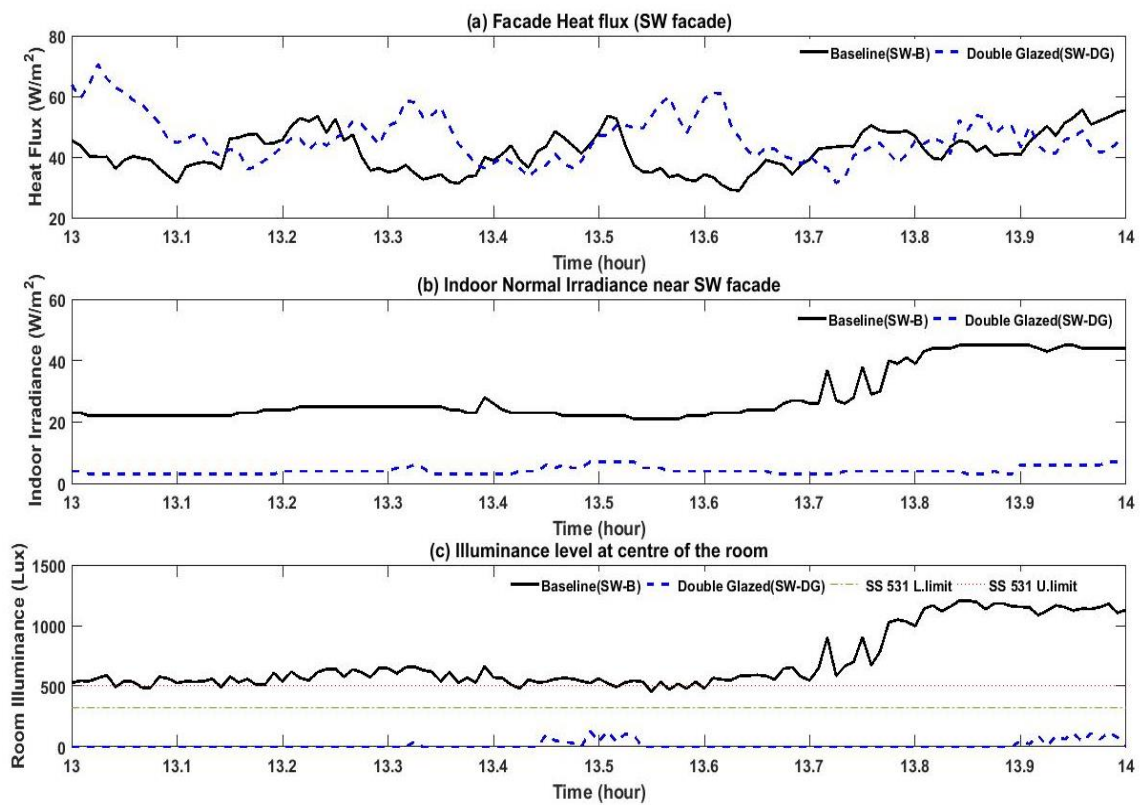


Figure 6. Comparative plots before and after retrofit double glazing of NW façade: (a) Façade heat flux; (b) indoor normal irradiance; (c) illuminance level at room center.

Table 6. Air-con power consumption and energy savings after retrofit double-glazing installation (measured values from test bedding).

Configuration Type/Name	Performance	Average Air-Con Power			
		9 a.m. to 12 p.m.	12 p.m. to 3 p.m.	3 p.m. to 6 p.m.	Whole Day
SE façade (no shade + clear SE façade)	Baseline	1.00 kW	N.A *	N.A *	N.A *
	DG	1.05 kW	-	-	-
SE façade (shade + clear SE façade)	Savings	-5%	N.A *	N.A *	N.A *
	Baseline	1.14 kW	1.29 kW	1.49 kW	11.76 kWh
SW façade (shade + clear SW façade)	DG	1.07 kW	1.23 kW	1.27 kW	10.69 kWh
	Savings	6%–7%	4%–5%	15%	9%–10%
NW façade (shade + solar film in NW façade)	Baseline	0.91 kW	1.09 kW	1.05 kW	9.15 kWh
	DG	0.9 kW	1.02 kW	0.96 kW	8.66 kWh
NW façade	Savings	1%	6%	8%–9%	5%–6%

N.A * indicates there were no comparable hourly zones with similar weather, for these cases.

The measured experimental observations for the SE façade is shown in Figure 4, which compares façade heat flux (into the room), indoor normal irradiance (measured near the SE façade), and room illuminance at the center of the room for 20 April (baseline, SE-B) and 6 April (double-glazed, SE-DG). The ambient conditions on 20 April, 11 a.m. to 12 p.m. (temperature, RH, total solar irradiance) were 32.4 °C, 55.7%, and 818 W/m², respectively. The corresponding ambient conditions during the same period on 6 April were 32.0 °C, 53.9%, and 523 W/m². Thus, the two chosen periods are quite comparable. Figure 4 depicts the reduction in room illuminance levels and indoor normal irradiance levels but with a significant increase in façade heat flux after retrofit double glazing, even though 6 April (double-glazed, SE-DG) had a slightly lower ambient solar radiation level during the period of comparison. The SE façade with clear glass and without protection from external sunshade receives significant heat gain from direct solar radiation during this period. The presence of a secondary glazing

layer with a low-e coating layer at position #3 reduces the direct solar transmission significantly, thereby resulting in lower lux and indoor irradiance values. However, the solar energy that is blocked by the low-e layer is re-radiated back into the ambient and into the room. The main advantage of this scenario was that it reduced the glare from the high lux level of 1454 to 486, which is within the recommended range [21]. As seen from Table 6, the net effect of increased façade heat flux and reduced direct solar transmission was that the heat gain was slightly higher during the direct sunshine period (9 a.m. to 12 p.m.). There were no very close comparable weather periods for the afternoon periods 12 p.m. to 3 p.m. and 3 p.m. to 6 p.m. The whole-day energy saving (arising from reduced HVAC energy consumption alone) for the SE clear façade during the observed test period was not very conclusive, due to the non-existence of similar days, but the overall change in power consumption was within the range of $\pm 1.5\%$.

The measured experimental observations for the SW façade is shown in Figure 5 by comparing the façade heat flux (into the room), indoor normal irradiance (measured near the SW façade), and room illuminance at the center of the room for 2nd May (baseline, SW-B) and 25th May (double-glazed, SW-DG). The ambient conditions on 2 May, 1 p.m. to 2 p.m. (temperature, R.H, total solar irradiance) were 31.1 °C, 63.3%, and 376 W/m², respectively. The corresponding ambient conditions during the same period on 25th May were 30.9 °C, 62.9%, and 307 W/m², implying that the two chosen periods are quite comparable. Figure 5 depicts the reduction in room illuminance levels and indoor normal irradiance levels but with a slight increase in façade heat flux after retrofit double glazing. The SW façade with clear glass and with protection from the external sunshade along with a more favorable solar angle, received a significantly lower heat gain from direct solar radiation compared to the SE façade. The presence of a secondary glazing layer with a low-e coating layer at position #3 reduces the direct solar transmission significantly, thereby resulting in lower lux and indoor irradiance values. However, the blocked solar energy at the low-e layer is re-radiated back into the ambient and into the room. However, the favorable solar angle and protection from the sunshade reduced the solar energy absorbed by the low-e layer, so the re-radiated energy is not significantly higher than in the baseline scenario. The main disadvantage of this scenario was it reduced the lux level from the useful range of 500–600 to a very low value of 10–60. As seen from Table 6, the net effect of slightly increased façade heat flux and significant reduction in direct solar transmission was that the heat gain was lower throughout the day. The whole-day energy saving (arising from reduced HVAC energy consumption alone) during the observed test period ranged from 9% to 10%.

The measured experimental observations for the NW façade is shown in Figure 6, which compares façade heat flux (into the room), indoor normal irradiance (measured near the NW façade), and room illuminance at center of the room for 17 June (baseline, NW-B) and 12 June (double-glazed, NW-DG). The ambient conditions on 17 June, 5 p.m. to 6 p.m. (temperature, R.H, total solar irradiance) were 31.1 °C, 61.9%, and 140 W/m², respectively. The corresponding ambient conditions during the same period on 12 June were 30.9 °C, 63.8%, and 175 W/m², implying that the two chosen periods are quite comparable. Figure 6 depicts the reduction in room illuminance levels and indoor normal irradiance levels, as well as the significant drop in façade heat flux, after retrofit double glazing. The NW façade had dual protection both from the existing solar film and from the external sunshade before the retrofit double glazing was installed. Even with unfavorable solar angle (as the sun shines normally into the façade from 3 p.m. to 6 p.m.), both the direct solar transmission and re-radiation of absorbed heat were significantly reduced. The solar film on the existing façade prevents a significant amount of thermal energy reaching the low-e layer, thereby reducing the consequent heating and re-radiation. However, the presence of a secondary glazing layer with a low-e coating layer at position #3 further reduces the direct solar transmission, thereby resulting in lower lux, indoor irradiance, and façade heat flux values. The main advantage of this scenario was that it reduced the façade heat flux significantly. (Lux levels are lower in the current comparison as the outdoor illuminance was low during the period of comparison for both the baseline and retrofit double-glazed scenario). As seen in Table 6, the net effect of decreased façade heat flux and significant reduction in direct solar transmission was that the heat

gain was lower throughout the day. The whole-day energy saving (arising from reduced HVAC energy consumption alone) during the observed test period ranged from 5% to 6%.

Table 6 presents the observed energy savings for the limited combination of scenarios tested for the days on which the test bedding was carried out. To obtain the annual energy savings and to also analyze other combinations of scenarios (arising from façade glass type, orientation, presence or absence of sun shade, and solar film), energy modelling simulations (as described in Section 4.2) were carried out and the results are tabulated in Table 7 and Figure 7. The light grey glass used in this simulation was a 10 mm thick glass with a Visible Light Transmissivity (VLT) of 0.483 and solar energy transmission of 0.383. The solar film has specifications as per Table 1. Table 7 confirms the conclusions made earlier that the net energy saving arising from the installation of low-e retrofit double glazing is more significant for scenarios where the existing façade is of tinted glass or for façades having a solar film installed. However, the absence of an external sunshade makes the retrofit double-glazing installation even more significant and compelling as, in these scenarios, the relative energy savings after retrofit double glazing is higher. With respect to directional dependence, the east- and west-facing façades benefit more from the retrofit double glazing, while the north- and south-facing façades have a slightly lower impact on the annual HVAC energy savings. The annual HVAC energy consumption is listed in Table 7 for each scenario by assuming that the yearly average Coefficient of Performance (COP) of the chiller-system is 2.5, both for the baseline scenario and for the glazed scenario. However, it is to be noted that the energy savings presented here as in Figure 7 are for the case modelled with only one glass façade with a window-to-wall ratio of 8% (i.e., glazing area accounts for 8% of the total surface area of the building envelope from all four sides). Thus, larger glass façades and/or multiple glass façades in a room will lead to larger energy savings.

Table 7. Annual energy savings from reduced air-con power consumption after retrofit double-glazing installation, derived from energy modeling simulations.

Orientation of Façade	Performance	Annual Air-Con Energy Consumption (kWh)				
		Clear Glass + Shade	Clear Glass + No Shade	Light Grey Glass + No Shade	Light Grey Glass + Shade	Clear Glass+Solar Film
East	Baseline	4901	5214	4933	4686	4441
	DG	4826	5104	4644	4461	4215
	Savings	1.5%	2.1%	5.9%	4.8%	5.1%
West	Baseline	4854	5139	4869	4647	4408
	DG	4787	5046	4606	4441	4205
	Savings	1.4%	1.8%	5.4%	4.4%	4.6%
South	Baseline	4563	4838	4622	4403	4247
	DG	4518	4766	4407	4248	4080
	Savings	0.98%	1.5%	4.7%	3.5%	3.9%
North	Baseline	4554	4857	4636	4397	4253
	DG	4510	4777	4414	4242	4083
	Savings	0.98%	1.65%	4.8%	3.5%	4%

Note: The savings are reported in percentage, which is the ratio of energy savings with respect to the corresponding baseline consumption.

In addition, in some scenarios where the daylight entering the room is too high and screens are used to avoid glare, and artificial lighting is subsequently used, the proposed solution can reduce glare and reduce the need for artificial lighting as well. It can result in energy savings through reduced lighting energy consumption, which has not been analyzed here, as it specific to the room type, orientation, and the activity involved in the room.

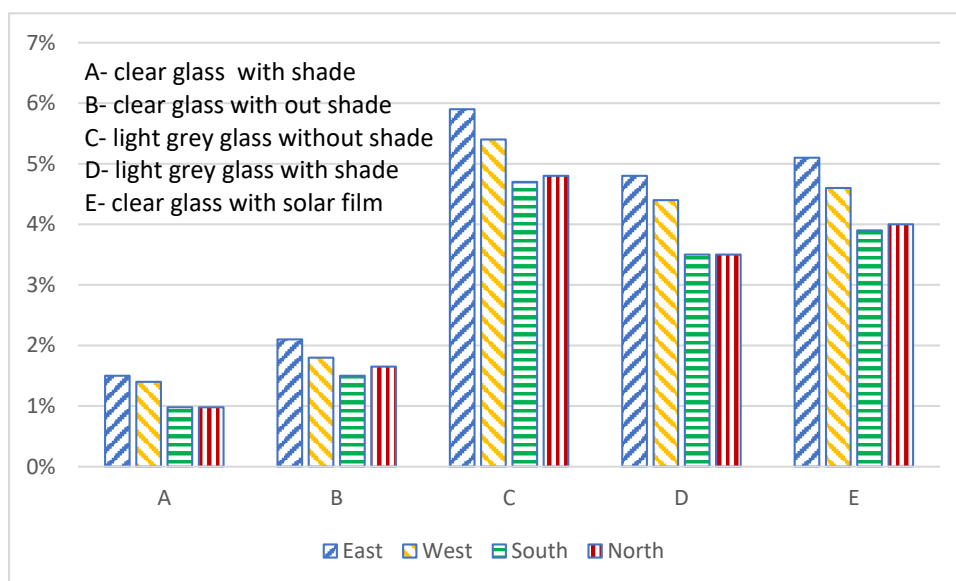


Figure 7. Annual energy savings % for different façades after retrofitting with low-e double glazing.

7. Conclusions

A quick and easy retrofit solution, using a secondary layer of low-e (hard coat) glass and installing as a retrofit double glazing in a non-sealed condition, was demonstrated and studied through real-life test-bedding. It was clear that low-e retrofit double glazing significantly reduced the visible light and direct solar transmission through the façade in all cases. However, the thermal heat flux (radiated and convected) from the façade into the room increased significantly in cases where the original façade is clear glass without any tint or solar film but did decrease in the tinted glass façades or in façades with solar film applied. Simulation models were built and used to analyze the annualized HVAC energy savings of various combinations of façade material and orientation. The east and west façade recorded the maximum HVAC energy savings. For the case of an east-facing tinted glass façade without any external sunshade, 5.9% savings in HVAC is achievable for a scenario with a 8% window-to-wall ratio (WWR defined relative to the total building envelope area). The results conclude that façades with tinted glass/solar films which are east/west-facing and without existing external sunshades should be the ideal choice for enhancement to low-e-based retrofit double glazing to improve the energy performance of existing buildings.

Author Contributions: Conceptualization, S.S and A.C.; methodology, A.C.; software, A.C.; validation, S.S, S.R.T. and A.C.; formal analysis, S.S.; investigation, S.S.; resources, A.C.; data curation, S.S.; writing—original draft preparation, S.S.; writing—review and editing, S.S.; visualization, S.S.; supervision, A.C.; project administration, S.S and A.C.; funding acquisition, A.C. All authors have read and agreed to the published version of the manuscript.

Funding: This research received no external funding.

Acknowledgments: The project was carried out as part of EPGC's internally funded project. AGC Asia Pacific Pte Ltd supplied and installed the hard coat low-e glass panels for every configuration sequentially. We thank AGC Asia Pacific Pte Ltd for their collaboration.

Conflicts of Interest: The authors declare no conflict of interest.

References

1. Energy Market Authority. *Singapore Energy Statistics (SES) Report*; Energy Market Authority: Singapore, 2018.
2. Building and Construction Authority. *BCA Building Energy Benchmarking Report*; Energy Market Authority: Singapore, 2014.
3. Thangavelu, S.R.; Myat, A.; Khambadkone, A. Energy Optimization Methodology of Multi-Chiller Plant in Commercial Buildings. *Energy* **2017**, *123*, 64–76. [[CrossRef](#)]

4. Quesada, G.; Rouse, D.; Dutil, Y.; Badache, M.; Hallé, S. A Comprehensive Review of Solar Facades. Opaque Solar Facades A Comprehensive Review of Solar Facades. Opaque Solar Facades. *Renew. Sustain. Energy Rev.* **2012**, *16*, 2820–2832. [[CrossRef](#)]
5. Quesada, G.; Rouse, D.; Dutil, Y.; Badache, M.; Hallé, S. A Comprehensive Review of Solar Facades. Transparent and Translucent Solar Facades. *Renew. Sustain. Energy Rev.* **2012**, *16*, 2643–2651. [[CrossRef](#)]
6. Hien, W.N.; Liping, W.; Chandra, A.N.; Pandey, A.R.; Xiaolin, W. Effects of Double Glazed Facade on Energy Consumption, Thermal Comfort and Condensation for a Typical Office Building in Singapore. *Energy Build.* **2005**, *37*, 563–572. [[CrossRef](#)]
7. Pérez-Grande, I.; Meseguer, J.; Alonso, G. Influence of Glass Properties on the Performance of Double-Glazed Facades. *Appl. Therm. Eng.* **2005**, *25*, 3163–3175. [[CrossRef](#)]
8. Planas, C.; Clemente, R.; Escalona, V.; Torres, M.; Alavedra, P.; Guzmán, A.; Cuerva, E. Headquarters of the Comisión Nacional Del Mercado de Valores. Double Façade Simulation Study. In Proceedings of the IBPSA 2007-International Building Performance Simulation Association, Beijing, China, 3–6 September 2007; pp. 156–160.
9. Valentín, D.; Guardo, A.; Egusquiza, E.; Valero, C.; Alavedra, P. Assessment of the Economic and Environmental Impact of Double Glazed Façade Ventilation Systems in Mediterranean Climates. *Energies* **2013**, *6*, 5069–5087. [[CrossRef](#)]
10. Fan, Y.; Xia, X. Energy-Efficiency Building Retrofit Planning for Green Building Compliance. *Build. Environ.* **2018**, *136*, 312–321. [[CrossRef](#)]
11. Luddeni, G.; Krarti, M.; Pernigotto, G.; Gasparella, A. An Analysis Methodology for Large-Scale Deep Energy Retrofits of Existing Building Stocks: Case Study of the Italian Office Building. *Sustain. Cities Soc.* **2018**, *41*, 296–311. [[CrossRef](#)]
12. Synnefa, A.; Vasilakopoulou, K.; De Masi, R.F.; Kyriakodis, G.E.; Londorfos, V.; Mastrapostoli, E.; Karlessi, T.; Santamouris, M. Transformation through Renovation: An Energy Efficient Retrofit of an Apartment Building in Athens. *Procedia Eng.* **2017**, *180*, 1003–1014. [[CrossRef](#)]
13. Michaelidou, M.; Dimitriou, S.; Christofi, M.; Katafygiotou, M.; Serghides, D.K. Energy Refurbishment Towards Nearly Zero Energy Multi-Family Houses, for Cyprus. *Procedia Environ. Sci.* **2017**, *38*, 11–19. [[CrossRef](#)]
14. van den Brom, P.; Meijer, A.; Visscher, H. Actual Energy Saving Effects of Thermal Renovations in Dwellings—Longitudinal Data Analysis Including Building and Occupant Characteristics. *Energy Build.* **2019**, *182*, 251–263. [[CrossRef](#)]
15. Rakhshan, K.; Friess, W.A. Effectiveness and Viability of Residential Building Energy Retrofits in Dubai. *J. Build. Eng.* **2017**, *13*, 116–126. [[CrossRef](#)]
16. Edeisy, M.; Cecere, C. Envelope Retrofit in Hot Arid Climates. *Procedia Environ. Sci.* **2017**, *38*, 264–273. [[CrossRef](#)]
17. Smith, N.; Isaacs, N.; Burgess, J.; Cox-Smith, I. Thermal Performance of Secondary Glazing as a Retrofit Alternative for Single-Glazed Windows. *Energy Build.* **2012**, *54*, 47–51. [[CrossRef](#)]
18. Somasundaram, S.; Chong, A.; Wei, Z.; Thangavelu, S.R. Energy Saving Potential of Low E-Coating Based Retrofit Double Glazing for Tropical Climate. *Energy Build.* **2019**. [[CrossRef](#)]
19. Somasundaram, S.; Raj Thangavelu, S.; Chong, A. Improving building efficiency using low-e coating based retrofit double glazing with solar films. *Appl. Therm. Eng.* **2020**. [[CrossRef](#)]
20. Singapore Standard Council, S. *Code of Practice for Air-Conditioning and Mechanical Ventilation in Buildings*; Singapore Standard Council, S: Singapore, 2016; Volume 2017, p. 62.
21. Singapore Standard. *SS 531: Code of Practice for Lighting of Work Places-Part 1: Indoor*; Singapore Standard: Singapore, 2006.

